MOLECULAR PHYSICS, 1995, VOL. 86, NO. 4, 857–864

Structure of variable-width square-well fluids from the reference hypernetted chain equation

By ALEJANDRO GIL-VILLEGAS†, CARLOS VEGA‡, FERNANDO DEL RÍO§ and ANATOL MALIJEVSKY‖

† Department of Chemistry, University of Sheffield, Sheffield S3 7HF, UK
‡ Departamento de Química Física, Facultad de Ciencias Químicas, Universidad Complutense, 28040 Madrid, Spain
§ Departamento de Física, Universidad Autónoma Metropolitana, Iztapalapa, Apdo 55-534, México, D.F. 09340, México
‖ Department of Physical Chemistry, Institute of Chemical Technology, CS-166 28 Prague 6, Czech Republic

(*Received 15 June 1995; accepted 12 July 1995*)

The problem of calculating the structure of square-well (SW) fluids in the context of non-conformal fluids is reviewed briefly. New and extensive results over a wide range of SW systems and thermodynamic states were obtained by means of the reference hypernetted chain (RHNC) integral equation. The results show that RHNC theory is in excellent agreement with the results of simulation, thus providing a reliable and fast procedure for obtaining the structure of fluids with discontinuous potentials. A few representative results are presented and compared with new Monte Carlo simulation data. The bridge functions obtained with the RHNC procedure are also compared with those calculated directly from the Monte Carlo radial distribution functions.

1. Introduction

The behaviour of simple models of non-conformal fluids (NCFs) has been of interest over the years due to their application in modelling colloids [1], investigating the dependence of liquid-phase stability on the range of the attractive forces [2, 3], and studying the effect of non-conformal changes in the liquid–vapour phase diagram [4, 5]. A class of fluids used widely to model NCFs is described by a system of spherical particles of diameter σ interacting with a potential of the form

$$u(r; \sigma, \epsilon, \lambda) = \begin{cases} \infty & r < \sigma \\ -\epsilon\phi(r, \lambda) & r \geqslant \sigma, \end{cases} \tag{1}$$

which consists of a hard-sphere-like repulsive interaction plus an attractive term $-\epsilon\phi(r)$. This last term is characterized by the depth ϵ of the well, and the parameter λ describing the range of the attractive forces. Changes in λ modify the shape of the potential, and hence produce a non-conformal variation in the system.

Typical models given by equation (1) and which have been studied extensively are the variable-width square-well (SW) and Yukawa fluids. Both interactions provide simple examples with both repulsive and attractive parts which furnish two important NCF limits: the adhesive hard spheres for very deep wells, $\epsilon \to \infty$, and short ranges λ, and the Kac limit for shallow wells, $\epsilon \to 0$, and $\lambda \to \infty$ [5]. The SW fluid has been used also as a reference system in perturbation and mapping theories of more realistic potentials [4, 6].

0026-8976/95 $10.00 © 1995 Taylor & Francis Ltd.

Because of this wide interest, the structure of SW fluids has been investigated amply by both computer simulation and integral equation methods. The results in the literature up to 1976 were reviewed by Barker and Henderson [7]. Up to that year, simulation studies concentrated on particular values of the SW range (almost all of them for $\lambda = 1{\cdot}5$) and hence did not exhibit the effects of non-conformal behaviour. Later, Henderson *et al.* [8] studied SW fluids with $1{\cdot}25 \leqslant \lambda \leqslant 2{\cdot}00$ by Monte Carlo simulations and perturbation theory. Molecular dynamics simulations for fluids with $1{\cdot}1 \leqslant \lambda \leqslant 3{\cdot}00$ have also been performed [9, 10]. The latter have been used to display NCF behaviour and in particular show that the SW fluid with $\lambda = 3{\cdot}0$ is already very close to the van der Waals limit [5, 10]. The liquid–vapour coexistence of variable width SW fluids has been investigated also using the Gibbs ensemble technique by Vega *et al.* [11], and its non-conformal thermodynamic behaviour analysed explicitly [5].

Simulation studies have played a very important role in developing and testing theories for the SW fluid, and in understanding the properties of this system. Simulations can nowadays be performed quite accurately but, in spite of the speed of present day computers, they are still too time consuming for several applications. On the other hand, perturbation theory for the structure of the SW fluids, i.e., for the radial distribution function $g_{sw}(r)$, has been shown to be rather inaccurate [8].

Integral equation theories for the SW fluid are the most extensively studied. Among those considered up to 1976 were the Percus–Yevick, the hypernetted chain (HNC), the mean spherical approximation (MSA), the optimized random phase approximation (ORPA), the exponential (EXP), and the linear exponential (LEXP) closures [7]. Of the simpler closures, the MSA appears to give the best results and the same relative virtue has been exhibited recently for SW fluid mixtures [12]. These integral equations are in many cases better than perturbation theory, and always much faster to use than simulations; nevertheless, they are still not accurate enough to give reliable information on non-conformal behaviour.

Analytical solutions within the MSA for the structure and thermodynamics of SW and Yukawa fluids have been obtained recently by Tang and Lu [13] for the SW case, and by Henderson *et al.* [14] for the Yukawa. These solutions are explicit in the density, temperature, and range λ, which make them adequate for applications like modelling the PVT diagram of real substances.

Although the MSA is suitable for applications where the knowledge of an analytical solution is more important than accuracy, when the latter is required the structural properties demand a better closure. The original version of the 'corrected' HNC equation, developed by Smith and Henderson [15] for the SW fluid with $\lambda = 1{\cdot}5$, showed a significant improvement in accuracy over the closures used previously. Later, the development of the reference hypernetted chain equation (RHNC) [16–19] opened the route to an accurate and fast calculation of $g(r)$. This equation has been proved to work very well for continuous potentials [20]. More recently, Lomba and Almarza [3] have shown that, in the Yukawa case, the liquid–vapour phase equilibria calculated with the RHNC equation are in excellent agreement with Gibbs ensemble simulation results.

In this short communication we show that the RHNC theory is also excellent for discontinuous potentials such as the SW of variable width and can hence be used with confidence to obtain the properties of this and similar NCFs. We display the accuracy of RHNC theory for the structure of SW fluids by comparing the $g_{sw}(r)$ obtained from it with Monte Carlo results. The virtues of RHNC theory for this

type of system are analysed further by comparing the bridge function obtained from the RHNC equation with that obtained by direct inversion of the MC $g_{sw}(r)$.

2. Theory

The radial distribution function of a fluid whose particles interact with the spherical intermolecular potential $u(r)$ is obtained from the total correlation function $h(r) = g(r) - 1$. The total correlation is obtained using the Ornstein–Zernike (OZ) equation

$$h(r_{12}) = c(r_{12}) + \rho \int \mathrm{d}\mathbf{r}_3 h(r_{13}) c(r_{23}), \tag{2}$$

where $c(r)$ is the direct correlation function. Usually, equation (2) is taken as the definition of $c(r)$. The OZ relation must be complemented by a further relation between the correlation functions and the intermolecular potential, i.e.,

$$c(r) = -\beta u(r) + h(r) - \ln h(r) + B(r), \tag{3}$$

an expression which involves a third function, the so-called bridge function $B(r)$. In order to close the set of equations (2) and (3) an approximation for $B(r)$ is required. The RHNC assumes that the bridge function has a universal shape described correctly by the hard-sphere bridge function [17]

$$B(r) = B_{HS}(r, \sigma). \tag{4}$$

The hard-sphere diameter σ needed in equation (4) is obtained by a minimum free-energy criterion [18] from

$$\int \mathrm{d}\mathbf{r}[g(r) - g_{HS}(r)]\sigma \left[\frac{\partial B_{HS}(r;\sigma)}{\partial \sigma}\right] = 0. \tag{5}$$

In this work we have used the parametrization of $B_{HS}(r)$ proposed by Malikevsky and Labík (ML), which gives [21]

$$B(r) = b^2(r), \tag{6}$$

where, for $x = r - 1 \leqslant a_4$,

$$b(r) = (a_1 + a_2 x)(x - a_3)(x - a_4)/a_3 a_4, \tag{7}$$

and, for $x > a_4$,

$$b(r) = A_1 \exp(-a_5(x - a_4)) \sin[A_2(x - a_4)]/r. \tag{8}$$

The parameters A_j are given in terms of the coefficients a_i, $i = 1, 6$. In the hard-sphere (HS) case, $a_i = a_i(\eta)$, where η is the packing fraction $\eta = \pi\rho\sigma^3/6$, and σ is the HS diameter.

3. Results

We solved the RHNC equation, given by equations (2)–(5), with the ML parametrization of $B_{HS}(r; \sigma)$ [21, 22]. Due to the discontinuity of the SW potential, a fine grid of 4096 points in the interval $[0, 5\sigma]$ was necessary. Then the OZ equation with the RHNC closure was solved using the numerical procedure due to Labík *et al.* [23].

We studied extensively 18 SW fluid systems with λ between 1·1 and 2·0. The densities ranged from $\rho^* = \rho\sigma^3 = 0{\cdot}05$ to $\rho^* = 0{\cdot}8$ or 0·9, and the temperatures from $T^* = kT/\epsilon = 0{\cdot}6$ to $T^* = 10$. In all of the one-phase states, and where independent simulation studies were available, the solutions of the RHNC equation are very close to the simulations. In all systems, the RHNC procedure did not have solutions close to the critical point, and deep within the liquid–vapour coexistence region (although solutions were found for some metastable states). Here, we present only a few selected results as an illustration. They are compared with new NVT Monte Carlo (MC) simulations performed with 256 particles and averaged over 15 million configurations. Figures 1–3 show the radial distribution function for three different SW systems, with values of λ commonly used in applications ($\lambda = 1{\cdot}3$, 1·5, and 1·8), and for densities typical of dense liquids. It can be seen from the figures that the agreement between the RHNC theory and the MC results is excellent. Similar or better agreement was found for all other SW ranges, temperatures, and densities.

A more precise and wider comparison is presented in table 1, which includes values of $g_{sw}(r)$ at $r = \sigma$ and $r = \lambda\sigma^+$, as well as the values of the pressure obtained from the virial equation. Deviations $\Delta g(r) = g_{RHNC}(r) - g_{MC}(r)$ are generally smaller than 1%; they reach a maximum of 1% at contact $r = \sigma$ and of 1·5% at $r = \lambda\sigma$, with similar behaviour for the pressure.

To test the adequacy of the RHNC theory further we calculated the bridge function $B_{sw}(r)$ from the simulated values $g_{MC}(r)$. This was done by assuming the same parametric form of Maliljevsky and Labík for $B_{sw}(r; a_i)$, equations (6–8), but considering the coefficients a_i as adjustable parameters. For given assumed values of a_i, $i = 1, 6$, the radial distribution function $g(r; a_i)$ was obtained by the procedure of Labík *et al.* [23]. The final values of the a_i for a given state and

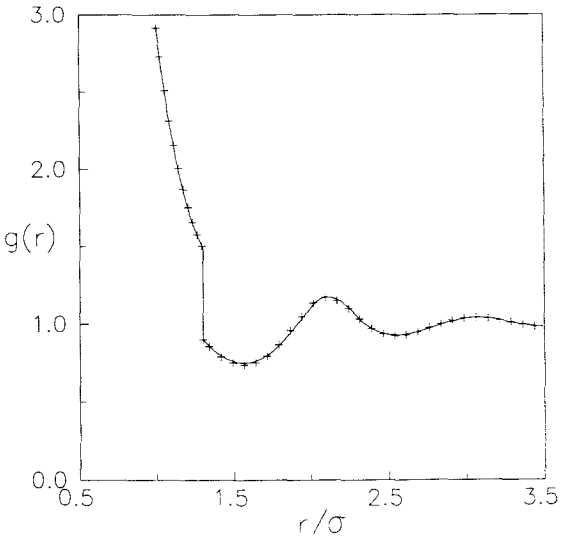

Figure 1. Comparison of theoretical and Monte Carlo radial distribution functions of a SW fluid with $\lambda = 1{\cdot}3$ at $\rho^* = 0{\cdot}7$ and $T^* = 2{\cdot}0$. The continuous curve is an interpolation of the MC results (the actual points are too close to be noticed at this scale), and + the RHNC results.

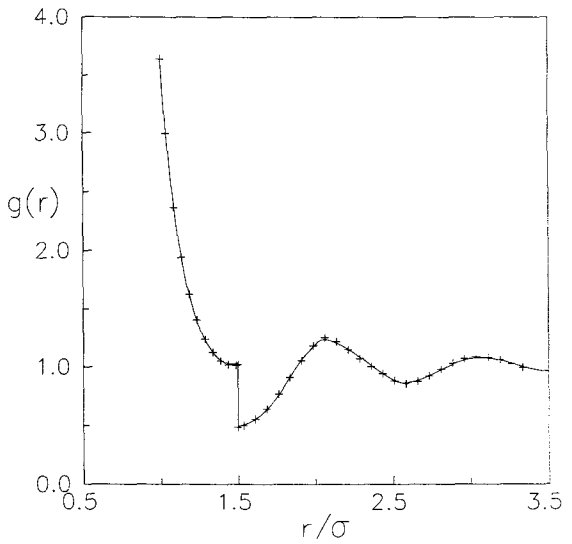

Figure 2. Comparison of theoretical and Monte Carlo radial distribution functions of a SW fluid with $\lambda = 1{\cdot}5$ at $\rho^* = 0{\cdot}8$ and $T^* = 1{\cdot}35$. Symbols have the same meaning as in figure 1.

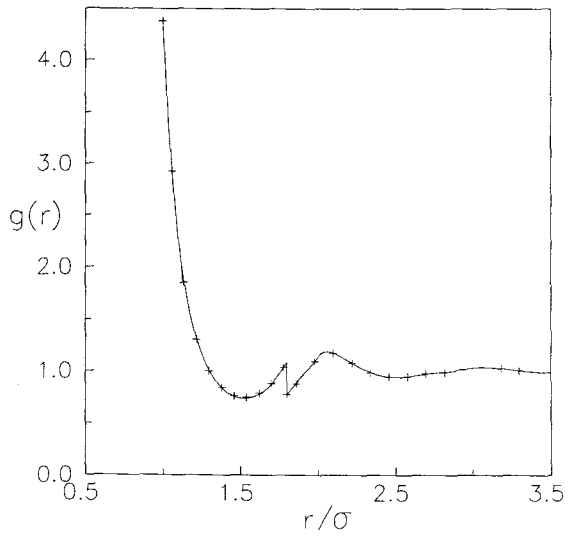

Figure 3. Comparison of theoretical and Monte Carlo radial distribution functions of a SW fluid with $\lambda = 1{\cdot}8$ at $\rho^* = 0{\cdot}8$ and $T^* = 3{\cdot}0$. Symbols have the same meaning as in figure 1.

system were then obtained by minimizing the square deviation

$$Q(a_i) = \sum_n \left[\frac{g_{MC}(r_n) - g(r_n; a_i)}{g_{MC}(r_n)} \right]^2.$$

This minimization procedure allowed us to obtain $g(r_n)$ within the uncertainty of the simulated $g_{MC}(r_n)$ in all cases (these are given in table 1). The functions $B_{sw}(r)$

Table 1. Comparison of contact values of $g_{sw}(r)$ and the compressibility factor $Z = PV/NkT$ for RHNC theory and Monte Carlo simulations. The values $g(\lambda)$ correspond to $r = \lambda\sigma^+$.

λ	ρ^*	T^*	$g_{MC}(\sigma)$	$g_{RHNC}(\sigma)$	$g_{MC}(\lambda)$	$g_{RHNC}(\lambda)$	Z_{MC}	Z_{RHNC}
1·3	0·7	2·00	2·914	2·919	0·901	0·903	3·389	3·393
		1·50	2·818	2·825	0·826	0·827	2·611	2·617
1·5	0·7	2·00	2·881	2·886	0·664	0·650	3·156	3·145
		1·50	2·777	2·783	0·596	0·589	2·311	2·285
		1·35	2·729	2·753	0·565	0·573	1·932	1·925
	0·8	10·00	3·983	4·008	0·691	0·691	7·262	7·305
		4·00	3·867	3·885	0·638	0·640	6·481	6·455
		2·00	3·749	3·753	0·559	0·562	5·232	5·227
		1·50	3·647	3·662	0·508	0·513	4·390	4·386
		1·35	3·643	3·639	0·487	0·493	4·081	4·038
1·8	0·7	3·00	3·365	3·398	0·745	0·746	3·412	3·458
	0·8	3·00	4·378	4·357	0·776	0·775	5·338	5·304

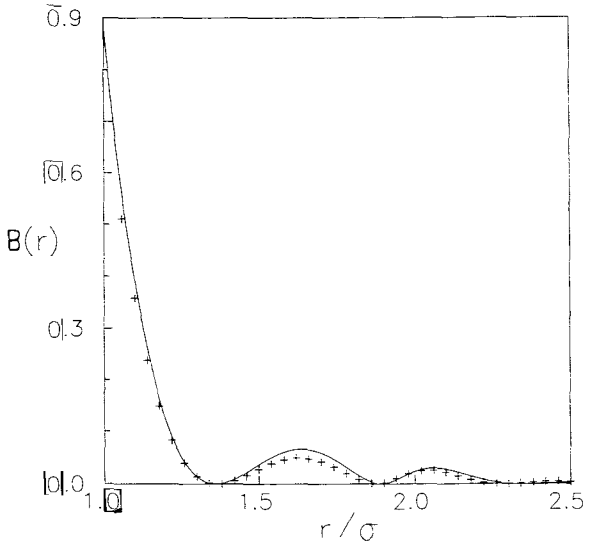

Figure 4. An example of a bridge function for the SW fluid. The continuous line is $B(r)$ from the RHNC theory, and + are the values from direct inversion of the MC $g(r)$. The system has $\lambda = 1{\cdot}8$, $\rho^* = 0{\cdot}8$ and $T^* = 3{\cdot}0$.

were found to be quite similar, but not identical to $B_{RHNC}(r)$. A typical comparison is shown in figure 4.

The differences between both bridge functions can be appreciated better when comparing the a_i coefficients used in the ML parametrization. In RHNC theory, a_i depend on the state variables through one single parameter: the HS diameter σ_{HS} determined from equation (5) and used in the packing fraction. This is not true for the bridge function obtained from the MC data, with adjustable parameters. Nevertheless, the latter were found to change smoothly and systematically with the state variables. Figures 5 and 6 show the change with temperature of these parameters

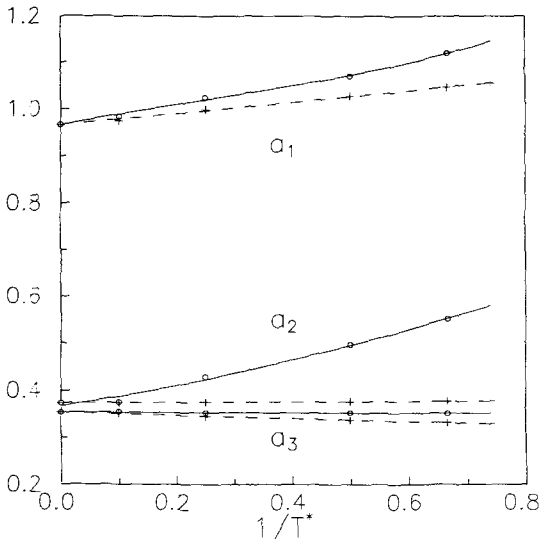

Figure 5. The temperature dependence of the first three bridge coefficients of the Malijevsky–Labík parametrization. The continuous curve represents the direct inversion of the MC data, and the dashed curves are the RHNC results. The SW system has $\lambda = 1{\cdot}5$ and $\rho^* = 0{\cdot}8$.

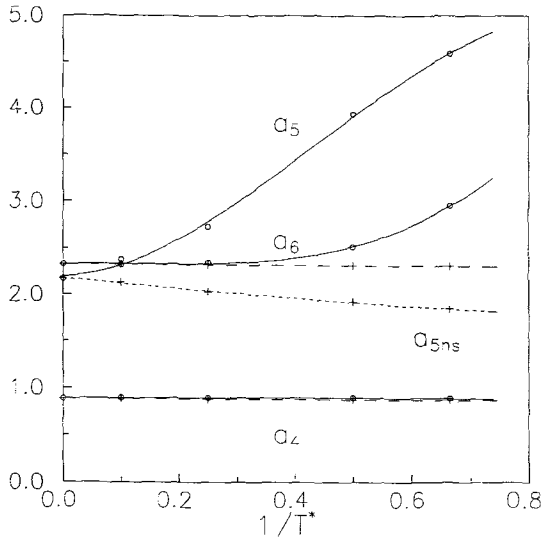

Figure 6. The temperature dependence of the first three bridge coefficients of the Malijevsky–Labík parametrization. The continuous curve represents the direct inversion of the MC data, and the dashed curves are the RHNC results. The SW system is the same as in figure 5.

in both cases. At high temperatures, where the SW fluid tend to behave like a HS system, the direct bridge functions tend to their RHNC value. The large differences in a_5 at higher densities affect only the rather small 'tail' of $B(R)$, and do not have a noticeable effect on $g(r)$. The systematic behaviour of σ_{HS} with ρ^* and T^* allows us to determine the RHNC results by parametrizing σ_{HS} in terms of the state variables.

4. Conclusion

We have shown that the optimized version of the RHNC [17–19] together with the ML parametrization of $B_{HS}(r; \sigma)$ [20, 21] provide an excellent description of the structure of SW fluids with $1{\cdot}1 \leqslant \lambda \leqslant 2{\cdot}0$. The high accuracy of the σ_{HS} obtained means that RHNC theory, with a fine enough grid, can be used with confidence in calculating the structure of fluids with discontinuous potentials with a considerable saving in time.

The bridge functions obtained with RHNC theory are very close to those obtained directly from Monte Carlo results for σ_{HS}. The fact that the effective diameters in the RHNC procedure vary smoothly with the thermodynamic state provides a further time-saving step in solving the integral equation.

This work was supported partially by the Consejo Nacional de Ciencia y Tecnología (México) project #0611-E9110.

References

[1] Poon, W. C. K., and Pusey, P. N., 1995, *Observation, Prediction and Simulation of Phase Transition in Complex Fluids*, NATO ASI series C, Vol. 460 (Dordrecht: Kluwer).
[2] Hagen, M. H. J., and Frenkel, D., 1994, *J. chem. Phys.*, **101,** 4093.
[3] Lomba, E., and Almarza, N. G., 1994, *J. chem. Phys.*, **100,** 8367.
[4] Gil-Villegas, A., Chávez, M., and Del Río, F., 1993, *Rev. Mex. Fís.*, **39,** 513.
[5] Gil-Villegas, A., Benavides, A. L., and Del Río, F., 1995, *Fluid Phase Equilibria*, in press.
[6] De Lonngi, D. A., and Del Río, F., 1985, *Molec. Phys.*, **56,** 691.
[7] Barker, J. A., and Henderson, D., 1976, *Rev. mod. Phys.*, **48,** 587.
[8] Henderson, D., Scalise, O., and Smith, W. R., 1980, *J. chem. Phys.*, **72,** 2431.
[9] Alejandre, J., private communication.
[10] Benavides, A. L., Alejandre, J., and Del Río, F., 1991, *Molec. Phys.*, **73,** 321.
[11] Vega, L., de Miguel, E., Rull, L. F., Jackson, G., and McLure, I. A., 1992, *J. chem. Phys.*, **96,** 2296.
[12] Del Río, F., Guzmán, O., and Malijevsky, A., 1995, *J. phys. Chem.*, **96,** 2296.
[13] Tang, Y., and Lu, B. C. Y., 1994, *J. chem. Phys.*, **100,** 6665.
[14] Henderson, D., Blum, L., and Nowortya, J. P., 1995, *J. chem. Phys.*, **102,** 4973.
[15] Smith, W. R., and Henderson, D., 1978, *J. chem. Phys.*, **69,** 319.
[16] Lado, F., 1973, *Phys. Rev.* A, **8,** 2548.
[17] Rosenfeld, Y., and Ashcroft, N. W., 1979, *Phys. Rev.* A, **20,** 1208.
[18] Lado, F., 1982, *Phys. Lett.* A, **89,** 196.
[19] Lado, F., Foiles, S. M., and Ashcroft, N. W., 1983, *Phys. Rev.* A, **28,** 2374.
[20] Talbot, J., Lebowitz, J. L., Waisman, E. M., Levesgue, D., and Weis, J. J., 1986, *J. chem. Phys.*, **85,** 2187.
[21] Malikevsky, A., and Labík, S., 1987, *Molec. Phys.*, **60,** 663.
[22] Labík, S., and Malijevsky, A., 1989, *Molec. Phys.*, **67,** 431.
[23] Labik, S., Malijevsky, A., and Vonka, P., 1985, *Molec. Phys.*, **56,** 709.